

Numerical strategies for the simulation of dissolution kinetics and fluid-dynamic instabilities in liquid couples with a miscibility gap

Marcello Lappa

MARS (Microgravity Advanced Research and Support Center), Via Gianturco 31,
80146, Napoli, Italy

e-mail: marlappa@marscenter.it, marlappa@unina.it

Abstract

This paper presents a numerical strategy for the simulation of phenomena disclosed by very recent experimentation within the framework of microscale studies devoted to the investigation of dissolution phenomena in liquid couples with a miscibility gap. Possible approaches to the problem are reviewed and discussed through a focused and critical comparison of similarities and differences, advantages, and intrinsic limitations. The proposed technique comes through major modification of existing volume tracking methods. Some effort is devoted to demonstrate its relevance when trying to capture the fluid-dynamic instabilities dependent on mechanisms at the liquid/liquid interface driven by non-equilibrium thermodynamic conditions.

1. Introduction

When a liquid system with a miscibility gap is cooled below the so-called “critical temperature”, it demixes into two liquids of different compositions and densities (the so-called minority and majority components) and phase separation occurs. Here “phase separation” stands for “spatial” separation of the phases; the thermodynamic counterpart of the process, i.e., the origin of decomposition in fact is a well-known and essentially understood chemical phenomenon since at least the mid-thirties of the last century. These behaviours are influenced by a number of possible phenomena (of different spatial extensions and temporal durations) pertaining to the fluid/fluid interface and/or its motion: nucleation and ensuing growth, Stokes sedimentation and

Marangoni migration, shape deformation, etc. (see, e.g., Lappa [1] and references therein). They have been finding increasing interest over recent years owing to their relevance for technological applications, and, accordingly, a number of mathematical models and methods have appeared for numerical/theoretical analysis of these aspects when they are disjoint or partially combined. For the sake of simplicity, non-miscible liquids (like oil and water) have often been selected as model fluids for fundamental studies concerning the sedimentation and migration phenomena; these particular aspects have been treated within the framework of volume of fluid (VOF, also referred to as “volume tracking”) techniques.

VOF-based simulations, however, are still very rare in the literature (rare and excellent efforts have been provided by Esmaeeli [2], Han and Tryggvason [3], Mehdi-Nejad et al. [4] in the case of droplet sedimentation; and Haj-Hariri et al. [5] in the case of Marangoni migration).

As discussed by Rider and Kothe [6], in fact, these techniques yet possess solution algorithms that are too often perceived as being heuristic and without mathematical formalism. Part of this misperception lies in the difficulty of applying standard hyperbolic PDE (partial differential equations) numerical analysis tools, which assume algebraic formulations, to methods that are largely geometric in nature (hence, the more appropriate term *volume tracking*). To some extent the lack of formalism in volume tracking methods, manifested as an obscure underlying methodology, has impeded progress in evolutionary algorithmic improvements and applications in particular to the case of systems with a miscibility gap. On the other hand, recent experimentation (Lappa et al. [7]) has shown that mechanisms somewhat related to the dissolution phenomena that can occur in these systems under particular conditions (system in non-equilibrium thermodynamic conditions) can be responsible for the onset of intriguing fluid-dynamic instabilities.

These instabilities represent a relevant aspect of the problem that should be taken into account in addition to the aforementioned migration and sedimentation mechanisms pertaining to the droplets. As gravitational sedimentation and Marangoni migration can be responsible for an irregular and non-uniform distribution of the minority phase within the majority phase (that is highly undesired for instance in technological processes related to the production of metal alloys), oscillatory fluid motion, in fact, can lead to detrimental effects induced by solute segregation.

Therefore, mass transfer across the surfaces separating phases with a miscibility gap should be regarded as a relevant part of research on these liquid systems, and there is an outstanding need for methods capable of taking into account these aspects. The problem is further complicated by the fact that special care is needed to properly capture a fluid-dynamic instability.

The alternative numerical approach, based on the so-called linear stability analysis, allows one to avoid the straightforward integration in time that would be required by volume of fluid methods as well as the solution of the Navier–Stokes equations in their complete and non-linear form.

The related mathematical treatment of the problem generally proceeds along the following lines: An initial flow that represents a stationary state of the system is considered. By supposing that the various physical variables describing the flow suffer small (infinitesimal) increments, the equations governing these increments are obtained. In obtaining these equations from the relevant equation of motion, all products and powers (higher than the first) of the increments are neglected while retaining only terms that are linear in them. Since stability means stability with respect to all possible (infinitesimal) disturbances, for an investigation on stability to be complete it is necessary that the reaction of the system to all possible disturbances be examined. This is accomplished by expressing an arbitrary disturbance as a superposition of certain basic possible modes and examining the stability of the system with respect to each of these modes. In practice, this approach considers all possible infinitesimal perturbations and usually provides better understanding of the instability mechanisms as well as more precise critical values of the governing parameters.

Despite the important capabilities offered to investigators by linear stability analyses, it should be stressed that the direct straightforward integration in time of the governing balance equations offers even more interesting advantages for the case under investigation here. This philosophy can provide, in principle, a wealth of additional aspects that could not be obtained on the basis of linear stability computations: the effective amplitude of the disturbances when they are saturated; the behaviour of the system far from the threshold point; a quite exhaustive picture of the subsequent stages of temporal evolution, etc. However, its capability to capture fluid-dynamic instabilities driven by surface processes is still an open question (with these methods, in fact, the interface separating the two liquids must be smeared over a region with a non-zero thickness) and must be proven.

Superimposed on these arguments is the fact that existing volume of fluid methods need to be modified (re-formulated) to account for interface motion (expansion or contraction) induced by solute absorption or release.

For these reasons, the present analysis has a two-fold purpose: it is devoted to (i) the introduction of a numerical approach based on the philosophy of volume tracking methods able to deal with the aforementioned surface dissolution kinetics; (ii) the assessment of its relevance when trying to capture the aforementioned fluid-dynamic instabilities.

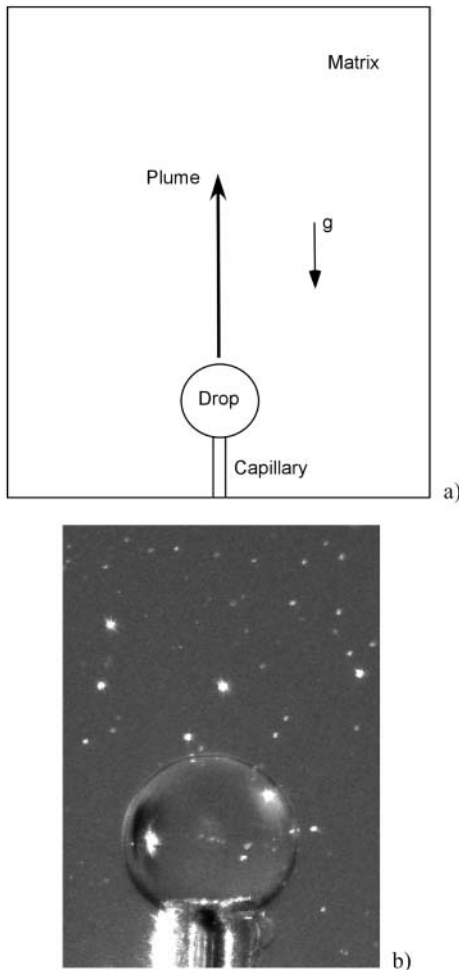


Figure 1 (a) Sketch of the geometrical configuration; (b) liquid drop at the tip of the capillary tube.

2. Numerical model

2.1. Basic assumptions

Figure 1 shows the geometry of the problem. A droplet of the minority phase is supposed to be anchored to the needle used to inject it into the external matrix. This prevents sedimentation and Marangoni migration phenomena. A thermodynamic constraint fixes the concentration jump between the interface sides. This jump, together with that of the concentration normal derivatives,

Table 1 Physical properties of the cyclohexane–methanol system.

| | |
|---|------------------------|
| D [$\text{m}^2 \text{s}^{-1}$] | 2×10^{-9} |
| ρ_1 [kg m^{-3}] | 0.782×10^3 |
| ρ_2 [kg m^{-3}] | 0.769×10^3 |
| v_1 [$\text{m}^2 \text{s}^{-1}$] | 1.03×10^{-6} |
| v_2 [$\text{m}^2 \text{s}^{-1}$] | 1.275×10^{-6} |
| β_{c1} [-] | -4.62×10^{-2} |
| β_{c2} [-] | 4.95×10^{-2} |
| β_{T1} [K^{-1}] | 1.14×10^{-3} |
| β_{T2} [K^{-1}] | 1.14×10^{-3} |
| C_{p1} [$\text{J kg}^{-1} \text{K}^{-1}$] | 2.51×10^3 |
| C_{p2} [$\text{J kg}^{-1} \text{K}^{-1}$] | 1.86×10^3 |
| λ_1 [$\text{J m}^{-1} \text{s}^{-1} \text{K}^{-1}$] | 2.02×10^{-1} |
| λ_2 [$\text{J m}^{-1} \text{s}^{-1} \text{K}^{-1}$] | 1.25×10^{-1} |
| σ_T [$\text{dyne m}^{-1} \text{K}^{-1}$] | 17.42 |

in turn, defines the entity of the dissolution cross-flow through the interface and the interface velocity relative to fluid.

Density and transport coefficients are assumed constant within each phase. The drop is bounded by a spherical liquid/liquid interface whose radius changes in time due to growth or dissolution. The hypothesis of spherical surface is acceptable if zero-g conditions prevail or, on the ground, if the volume of the liquid drop is small (few millimetres), and/or if the density difference between the two phases is very small. The couple cyclohexane–methanol is considered as reference liquid system with a miscibility gap since this couple is transparent to visible light, the critical temperature is close to ambient temperature, and the two liquids have very similar densities (see Table 1).

2.2. Phase field model

In a phase-field model (volume tracking philosophy), a phase-field variable ϕ that varies in space and time is introduced to characterise the phase. In place of the ‘sharp’ transition from one phase to the other, the phase-field varies smoothly but rapidly through an interfacial region. The effect is a formulation of the free boundary problem that in principle does not require application of interfacial conditions at the unknown location of a phase boundary.

In the specific case of drops growing or dissolving in a matrix of different liquid, one must generally accomplish at least two things simultaneously: (i) determine the concentration fields in both the liquid phases and (ii) determine the position of the interface between phase 1 and phase 2.

2.3. Volume of fluid method for dissolving drops

It is a single region formulation and allows a fixed-grid solution to be undertaken. It is therefore able to utilise standard solution procedures for the fluid flow and species equations directly, without resorting to mathematical manipulations and transformations.

The model is based on the mass balance equations. The diffusion of the species is governed by the equations (drop = phase 1 $\rightarrow \phi = 1$, matrix = phase 2 $\rightarrow \phi = 0$):

$$\frac{\partial C_1}{\partial t} = [-\underline{\nabla} \cdot (\underline{V} C_1) + D \nabla^2 C_1] \quad \text{if } \phi = 1, \quad (1)$$

$$\frac{\partial C_2}{\partial t} = [-\underline{\nabla} \cdot (\underline{V} C_2) + D \nabla^2 C_2] \quad \text{if } \phi = 0, \quad (2)$$

where D is the binary interdiffusion coefficient and C_1 and C_2 are the concentrations of one of the two components (for the present case it is methanol) in the minority (drop) and majority (matrix) phases, respectively. The initial constant concentrations in the drop and in the matrix are denoted by $C_{1(o)}$ and $C_{2(o)}$, respectively (for the case under investigation: $C_{1(o)} = 1$, i.e., drop of pure methanol, and $C_{2(o)} = 0$, i.e., matrix of pure cyclohexane).

The behaviour of the two phases is coupled through the equilibrium concentration values imposed on the two sides of the interface. These values come from the miscibility law (see, e.g., Figure 2 for the couple methanol–cyclohexane) according to the local value of the temperature of the interface (for isothermal conditions of course the equilibrium values are constant along

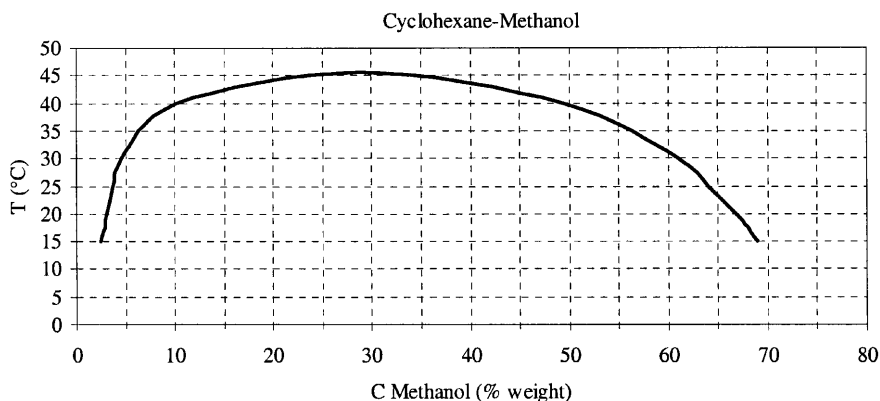


Figure 2 Phase diagram for the cyclohexane–methanol system.

the interface). At the interface ($0 < \phi < 1$), the concentrations must satisfy the equilibrium conditions:

$$C_1|_i = C_{1(e)}(T) \quad (3)$$

$$C_2|_i = C_{2(e)}(T) \quad (4)$$

Equations (3) and (4) rely on the assumption that equilibrium at the liquid/liquid interface is attained instantaneously (see Perez De Ortiz and Sawistowski [8]). They behave as “moving boundary conditions”.

Note that, as mentioned before, in place of the ‘sharp’ transition from one phase to the other that would characterise the multiple region formulations (in that case the interface separating the bulk phases is a mathematical boundary of zero thickness), here the phase-field varies smoothly but rapidly through an interfacial region whose thickness is not zero. This region, defined by the mathematical conditions $|\nabla\phi| \neq 0$, $0 < \phi < 1$, moves through the computational domain according to the behaviour of the different phases (i.e., according to the behaviour of ϕ).

The flow is governed by the continuity equation and Navier–Stokes equations:

$$\nabla \cdot \underline{V} = 0, \quad (5)$$

$$\frac{\partial(\rho\underline{V})}{\partial t} = -\nabla p - \nabla \cdot [\rho\underline{V}\underline{V}] + \nabla \cdot [\mu(\nabla\underline{V} + \nabla\underline{V}^T)] + \underline{F}_{Ma} + \underline{F}_g, \quad (6)$$

where

$$\rho = \rho_{1(o)}\phi + \rho_{2(o)}(1 - \phi), \quad (7a)$$

$$\mu = \mu_1\phi + \mu_2(1 - \phi). \quad (7b)$$

In the last term of Eq. (6) we have

$$\begin{aligned} \underline{F}_g = & \rho g [\beta_{C1}(C_1 - C_{1(o)})]\phi + \rho g [\beta_{C2}(C_2 - C_{2(o)})](1 - \phi) \\ & + \rho g [\beta_{T1}(T - T_{(o)})]\phi + \rho g [\beta_{T2}(T - T_{(o)})](1 - \phi), \end{aligned} \quad (7c)$$

i.e., the Boussinesque approximation is used to model the buoyancy forces. Also, β_{c1} and β_{c2} are the solutal expansion coefficients related to the mutual interpenetration of the phases (1) and (2), and β_{T1} and β_{T2} are the thermal expansion coefficients. The source term \underline{F}_{Ma} takes into account the other driving force involved in the phenomena under investigation, i.e., the Marangoni effect.

The strategy used herein to account for this force, in fact, is based on the continuum surface force (CSF) and continuum surface stress (CSS) models (see the discussion below).

In the light of the well-known Young–Laplace equation, the surface tension can be written simply in terms of a pressure jump across the surface. This force, in turn, can be expressed as a volume force in Eq. (6) using the divergence theorem or a similar artifice to replace the surface force with a volume force. The end of the story is that the interfacial surface forces can be incorporated as body forces per unit volume in the momentum equations rather than as boundary conditions. Instead of a surface tensile force boundary condition applied at a discontinuous interface of the two fluids, a volume force can be used that acts on fluid elements lying within a transition region of finite thickness. This also means that the CSF formulation makes use of the approach that discontinuities can be approximated, without increasing the overall error of approximation, as continuous transitions within which the fluid properties vary smoothly from one fluid to the other over a distance of $O(h)$, where h is a length comparable to the resolution of the computational mesh. Surface tension, therefore, is felt everywhere within the transition region through the volume force included in the momentum equations. A similar mathematical treatment is possible for the contribution related to surface tension gradients along the interface (Marangoni stress).

It is known in fact that the expression for the stress jump \underline{f} , across the interface is given by (see the elegant formalism of Haj-Hariri et al. [5]):

$$\underline{f} = \left[\sigma K \underline{\hat{n}} - \frac{\partial \sigma}{\partial T} (\underline{I} - \underline{\hat{n}} \underline{\hat{n}}) \cdot \underline{\nabla} T \right], \quad (8)$$

where $\underline{\hat{n}}$ is the unit vector perpendicular to the fluid/fluid interface $\underline{\hat{n}} = -\frac{\underline{\nabla} \phi}{|\underline{\nabla} \phi|}$, σ is the surface tension, K is the curvature ($K = 2/R$ in the case of a spherical surface with radius R), and \underline{I} is the identity matrix.

The surface force per unit interfacial area should be added in the momentum equation as $\underline{f} \delta$, where δ is the Dirac-pulse function used to localise the force explicitly at the interface. As previously discussed, it can formally be replaced by its volume-distributed counterpart, \underline{F} , which satisfies

$$\int_{-\infty}^{\infty} \underline{F}(s) ds = \int_{-\infty}^{\infty} \underline{f}(s) \delta(s) ds, \quad (9)$$

where (s) is a level-set function denoting the normal distance from the interface (the interface corresponds to $s = 0$) and $\delta(s)$ is the Dirac delta function

with its singularity on the interface. Rigorously speaking, f is not defined for non-zero s and must be extended appropriately (e.g., it can be assigned a value of zero for nonzero s because of the presence of the delta function). A comparison of the two integrals in Eq. (9) suggests $\underline{F} = \underline{f} \cdot \delta(s)$. Although this expression is of little value in its present form, much can be gained from it if a mollified delta function is used, consistent with the smearing of the interface. Recognising that

$$\int_{-\infty}^{\infty} \delta(s) ds = \int_{-\infty}^{\infty} \hat{n} \cdot \underline{\nabla} \phi ds = 1, \quad (10)$$

the mollified delta function can be defined as $|\underline{\nabla} \phi|$, which, in turn, leads to $\underline{F} = \underline{f} |\underline{\nabla} \phi|$.

Thus the second source term in Eq. (6) reads

$$\underline{F}_{Ma} = \left[\frac{2\sigma}{R} \hat{n} - \frac{\partial \sigma}{\partial T} (\underline{I} - \hat{n}\hat{n}) \cdot \underline{\nabla} T \right] |\underline{\nabla} \phi|, \quad (11)$$

where, as previously discussed in the light of the Young–Laplace equation, the first term in the square parenthesis is the normal stress contribution responsible for the shape equilibrium in perpendicular direction, whereas the second is the Marangoni shear stress along the surface that can be responsible for the Marangoni surface phenomena.

The temperature distribution is governed by the energy equation:

$$\frac{\partial \rho C_P T}{\partial t} = [-\underline{\nabla} \cdot (\rho C_P \underline{V} T) + \underline{\nabla} \cdot (\lambda \underline{\nabla} T)], \quad (12)$$

where the thermal conductivity λ and the specific heat C_P are computed as

$$\lambda = \lambda_1 \phi + \lambda_2 (1 - \phi), \quad (13a)$$

$$C_P = C_{P1} \phi + C_{P2} (1 - \phi). \quad (13b)$$

The core of this method is its technique for adjourning ϕ . The tracking of the interface between the phases is accomplished by the solution of a special continuity integral equation for the volume of the liquid drop taking into account the release or absorption of solute through the interface (the liquid drop is assumed to be a sphere of radius R increasing due to growth or decreasing due to dissolution).

The jump specie balance equation reads

$$-D \frac{\partial C_2}{\partial n} \Big|_i + C_2|_i \dot{m} = -D \frac{\partial C_1}{\partial n} \Big|_i + C_1|_i \dot{m}, \quad (14a)$$

where \dot{m} is the mass flow rate through the interface (n points towards the matrix; if the drop dissolves, \dot{m} is positive and $\frac{dR}{dt}$ is negative, i.e., $\dot{m} = -\frac{dR}{dt}$); therefore, integrating over the surface of the drop, one obtains for the time evolution of the radius

$$\frac{dR}{dt} = D \frac{1}{S} \oint \frac{1}{C_1|_i - C_2|_i} \left(\frac{\partial C_2}{\partial n} \Big|_i - \frac{\partial C_1}{\partial n} \Big|_i \right) dl, \quad (14b)$$

where S is the surface of the drop, and $\frac{\partial C}{\partial n} = \nabla C \cdot \hat{n}$.

After the computation of the radius at the new instant ($n + 1$), then the distribution of the phase variable ϕ is re-initialised to take into account the volume change, i.e., $\phi = 1$ for $r < R$ and $\phi = 0$ for $r > R$.

Equations (1), (2), (5), (6), (12), and (14b) represent a system of five partial differential equations and one ordinary differential equation whose solution governs the non-linear behaviour of the physical system under investigation.

Note that the present mathematical model and related numerical technique can be regarded as a very hybrid volume of fluid method.

In the ‘‘classical’’ VOF methods, the phase field variable ϕ is ‘‘advected’’, solving an appropriate partial differential transport equation; this formulation has been often used for the solution of typical problems dealing with the migration of bubbles or drops in liquids. It relies on the fact that the fluids are not interpenetrating. For the present method, the equation governing the evolution of ϕ comes from mass balance conditions rather than from transport. Moreover, interpenetration of the different fluids is allowed according to the coupled behaviour of Eqs. (1), (2), and (14b).

Furthermore, Eq. (14b) provides the necessary coupling among the species and momentum equations. The density and the dynamic viscosity of the liquid in Eq. (6) in fact are computed according to the instantaneous distribution of ϕ . Additional coupling between the species and momentum equations is due to the volume force term (Boussinesque approximation) in Eq. (6).

Equations (1), (2), (5), (6), (12) can be solved with the SMAC method. The method is not described here for the sake of brevity and since it is well-known. For further details, see, e.g., [9, 10].

3. Validation through comparison with experiments

If a temperature gradient is imposed along the gravity direction (x coordinate) by heating from above the test cell filled with the matrix liquid, the numerical method described in Section 2 “captures” the fluid-dynamic oscillatory instabilities disclosed by previous experimental investigation [7]. As an example, Figure 3 shows the good agreement between the computed instability threshold and the corresponding experimental values for different initial droplet volumes. Grid convergence, however, requires a very large number of computational points to be obtained (a grid of 400×100 is necessary for a $[4 \times 10^{-2} \text{ (m)}] \times [1 \times 10^{-2} \text{ (m)}]$ test cell).

Figure 4 illustrates typical spatio-temporal behaviours pertaining to the instability. Instead of a steady regular buoyant plume, release of solute occurs in the form of discrete events separated by certain time (and thus space) intervals. The instability in fact leads somehow to a “periodic shooting” of a “packet” of lighter fluid in the surrounding liquid. This behaviour appears in the form of a couple of curls that are initially formed close to the drop surface and then are transported upwards by buoyancy effects (see the experimental results in Figure 5).

The phenomenon can also be seen as a disturbance travelling towards the top (i.e., a perturbation of the solutal and flow field periodically rising along the

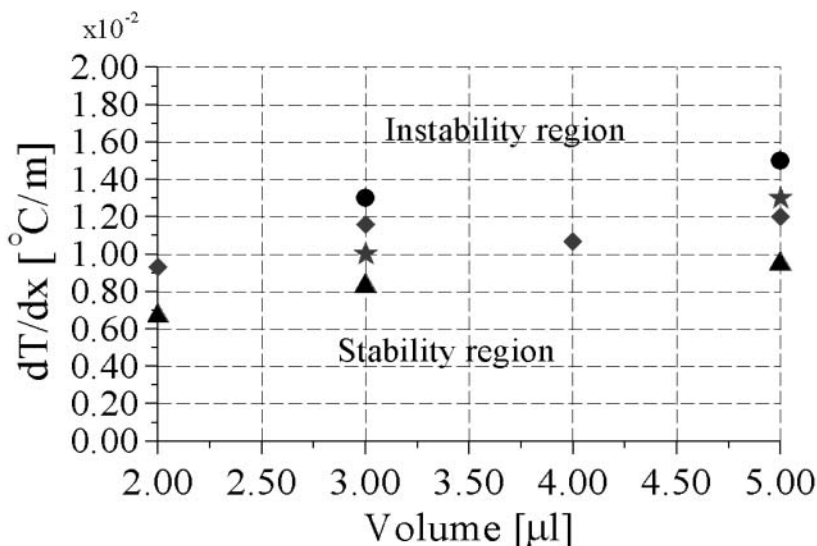


Figure 3 Stability map and critical temperature gradient ($\partial T/\partial x$) as a function of the initial droplet volume (numerical and experimental results). The critical threshold is an increasing function of the initial volume. ▲, exp. res. (stable); ◆, exp. res. (unstable); ★, num. res. (stable); ●, num. res. (unstable).

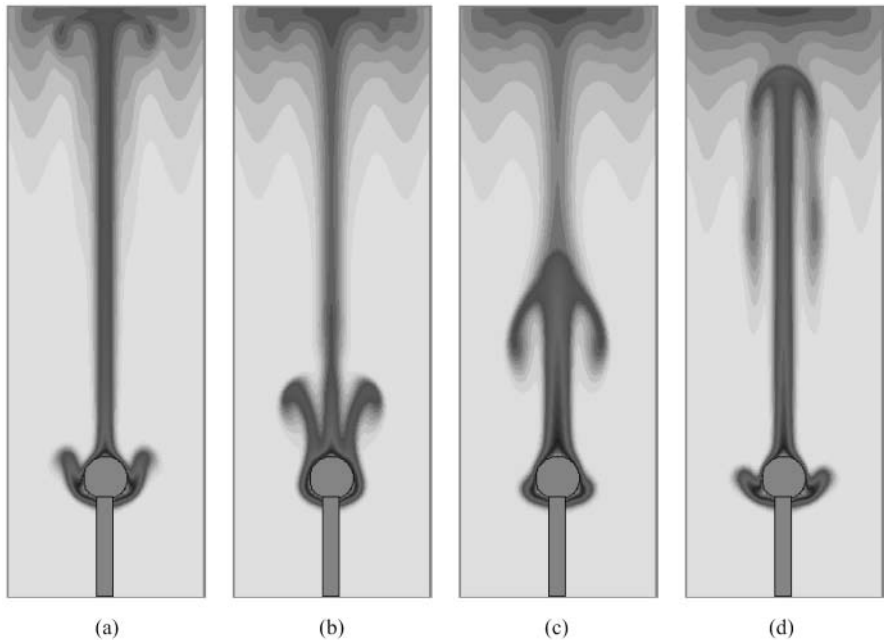


Figure 4 Computed evolution of the unstable solutal plume: concentration and flow field patterns for a 5- μl droplet of methanol dissolving into a matrix of cyclohexane with $\partial T/\partial x = 1.5 \times 10^2$ [$^{\circ}\text{C m}^{-1}$] ($T_{\text{average}} = 27^{\circ}\text{C}$): one period of oscillation is shown ($\tau = 26$ s) by means of subsequent snapshots.

symmetry axis). With regard to its origin, many elements seem to support the idea that it is a mechanism of gravitational nature. In the absence of gravity and related buoyancy forces, this type of instability, in fact, is suppressed.

Along these lines, studies pertaining to the case of moving droplets of methanol dissolving within a matrix of cyclohexane (same couple of liquids treated in the present paper) under microgravity conditions were carried out by Bassano [11]. According to such studies, obtained within the framework of a level-set moving boundary method, in 0-g conditions, a droplet of methanol subject to the effect of a temperature gradient simply migrates within the external matrix of cyclohexane while dissolving and deforming under the effect of shear stresses induced by the motion. In such a case, no fluid-dynamic instabilities arise; this can be regarded as an indirect but clear demonstration of the fact that the present instability is somewhat related to the interplay between buoyancy and surface tension forces.

In reality, a clear evidence of the counteracting behaviour responsible for the onset of the present instability is given by the presence along the drop surface of a “detachment point” (Figure 6). This point corresponds to the detachment of the layer of liquid transported close to the interface by thermal

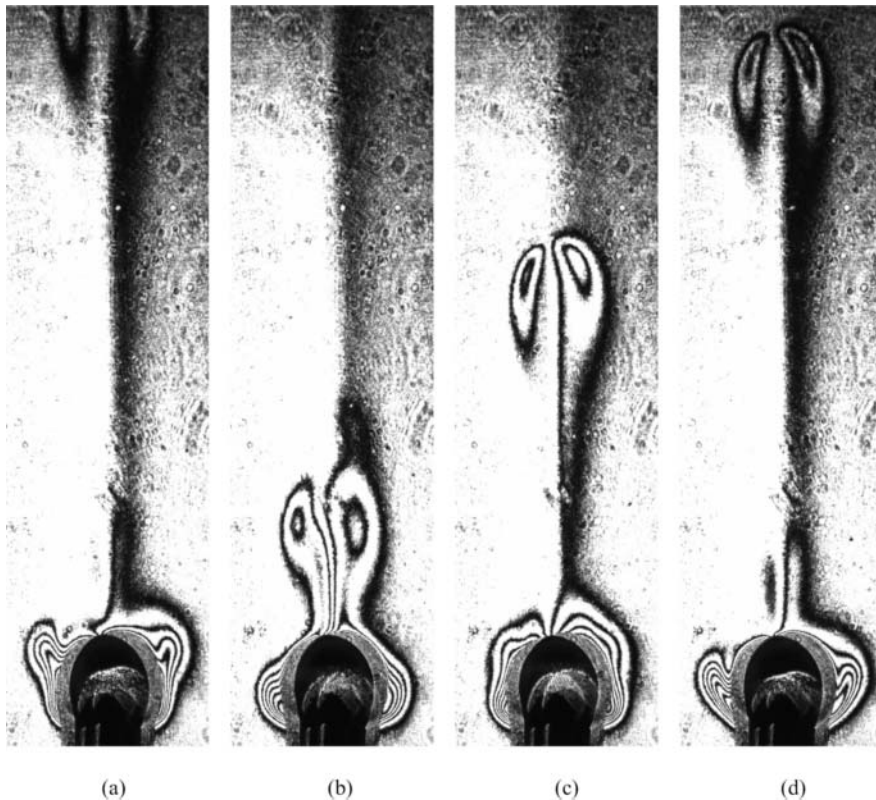


Figure 5 Experimental evolution of the unstable solutal plume: concentration and flow field patterns for a 5- μl droplet of methanol dissolving into a matrix of cyclohexane with $\partial T/\partial x = 1.5 \times 10^2$ [$^{\circ}\text{C m}^{-1}$] ($T_{\text{average}} = 27^{\circ}\text{C}$): one period of oscillation is shown ($\tau = 26$ s) by means of subsequent snapshots.

surface tension forces. Owing to the solutal buoyancy forces that oppose to downward motion, the surface layer has not enough momentum to reach the rear of the drop (this phenomenon exhibits an outstanding theoretical kinship with the corresponding phenomenon, well known by aerospace engineers, characterising the separation of air boundary layers from thin wing airfoils).

For this reason, return flow is initiated prior to reaching the drop base. Since the detached layer is lighter than the liquid matrix, not far away from the drop, the buoyancy forces tend to bring this fluid towards the top. Thus, the restoring upward force exerted by the stabilising solutal density gradients on the downward-flowing hot fluid, restricts the flow (downward motion and return rising flow) to an area close to the drop. In other words, the surface transfers warm liquid from the peak of the drop to the lower regions until at a certain stage (the detachment point) solutal buoyancy and continuity bring the fluid up again, resulting in a closed toroidal vortex (this also means that



Figure 6 Experimental evidence of “detachment points” along the drop surface.

the generation of curls close to the drop surface is strictly related to the counteracting behaviour of buoyancy and surface-tension forces; it is the direct opposition of these forces that leads to the production of vorticity). Of course, the detachment point does not hold a fixed position, but continuously undergoes rising and descending motion along the drop surface according to the alternate direction of the surface flow driven by the opposing forces mentioned before. Such behaviour is strictly associated with a periodic release of toroidal convection rolls in the region around/above the dissolving drop (i.e., it is responsible for the “continuous” production of vorticity that corresponds to the aforementioned rise of curls).

The consistency of numerical predictions with experimental data suggests that rate-controlling steps are well captured by the present numerical method and related philosophy.

With regard to this aspect, finally, it should be mentioned that the possible simulation of the present dynamics by means of moving-boundary approaches like that used by Bassano [11] would represent a ill-posed problem owing to the fact that the droplet is locked to its initial position and the solution of a phase advection equation is not suitable for the treatment of such a condition.

4. Comparison with other results

Many recent experimental studies pointed out that surfactants may also play a crucial role in creating interfacial instabilities in binary liquid–liquid systems and oscillation (referred to as “kicking” by these authors) of drops (see, e.g., Perez de Ortiz and Sawistowski [12], Liang and Slater [13], Bekki et al. [14, 15]).

The effect of surfactants on interfacial mass transfer in binary liquid–liquid systems (dissolving drops) was experimentally investigated more recently by Agble and Mendes Tatsis [16] using the Schlieren and the Mach-Zehnder optical techniques. The experiments were focused on the analysis of interfacial stability by means of direct examination of the interface of a drop of an organic phase (saturated with water) which was immersed in an aqueous phase of pure water. The onset of Marangoni convection and of possible fluid-dynamic instabilities at the interface was clearly observed. The role played by the surfactants (these substances can alter the surface tension) in inducing possible surface instabilities was investigated in detail in a subsequent analysis (Agble and Mendes Tatsis [17]). In this analysis, much room was devoted to comparing the available experimental results with canonical and/or semi-empirical surface stability criteria introduced over the years for the case of various binary liquid/liquid interfaces in the presence of a transferring surfactant; i.e., the Sternling and Scriven [18] criteria for ternary systems, the Hennenberg et al. [19, 20] criteria for surfactant transfer, the semi-empirical criteria of Nakache et al. [21]. It was found that these criteria often fail in predicting the observed phenomena. Along these lines, it is our opinion that many of the phenomena mentioned above in the case of added surfactants could be explained according to the present model where the instability is induced by the counteracting action of buoyancy and surface tension forces, the thermal surface tension gradient being simply replaced by the effect of the concentration gradient of surfactant for the cases above.

The present model could also explain other similar phenomena that have been observed even in the absence of surfactants and imposed thermal gradients.

For instance, many authors (see, e.g., the pioneering analysis of Lewis and Pratt [22]) observed rippling and erratic pulsations at the interface of drops of organic solvents dispersed in various solvents. In reality, during the related mass transfer process, interfacial tension gradients (originated owing to temperature gradients produced by the heats of solution) may be created at the interface and may cause the onset of Marangoni convection leading to the oscillatory mechanism elucidated in Section 3.

5. Conclusions

In light of the foregoing discussions, it can be concluded that the choice of a volume tracking numerical philosophy is appropriate for the problem under investigation, despite the very limited number of analyses in the literature where this philosophy was used for the investigation of interface dynamics and of problems where the interface plays a critical role in the onset of fluid-dynamic instabilities (see, e.g., the analyses dealing with the convective instabilities in falling liquid jets of Konkachbaev and Morley [23] and of Tryggvason et al. [24]).

Beyond these numerical/theoretical aspects, the case treated in this article, about the pulso-oscillatory flow originated from a droplet locked to its initial position at the bottom of a test cell, can be regarded as a relevant model for the study of the fascinating phenomena that can occur during the technological processing (cooling) of immiscible metal alloys when the droplets created by the thermodynamic phase-separation process tend to settle to the bottom of the container and, therefore, to be clustered in a zone at a different temperature where they are no longer in thermodynamic equilibrium with respect to the surrounding liquid.

Acknowledgements

The author would like to thank Dr. L. Carotenuto (MARS) for some helpful information, Dr. C. Piccolo (MARS) for providing many data about the experimental results, and Dr. E. Bassano (MARS) for the useful discussion about the application of level-set numerical methods to the general case of moving and deforming droplets.

References

- [1] Lappa, M., Assessment of VOF strategies for the analysis of Marangoni migration, collisional coagulation of droplets and thermal wake effects in metal alloys under microgravity conditions, *Comput. Mat. Continua*, 2 (2005), 51–64.
- [2] Esmaeeli, A., Phase distribution of bubbly flows under terrestrial and microgravity conditions, *Fluid Dynam. Mater. Processing*, 1 (2005), 63–80.
- [3] Han, J., Tryggvason, G., Secondary breakup of axisymmetric liquid drops. I. Acceleration by a constant body force, *Phys. Fluids*, 11 (1999), 3650–3667.
- [4] Mehdi-Nejad, V., Mostaghimi, J., Chandra, S., Two-fluid heat transfer based on a volume tracking advection algorithm, 9th International Conference on Liquid Atomization and Spray Systems, 2003.
- [5] Haj-Hariri, H., Shi, Q., Borhan, A., Thermocapillary motion of deformable drops at finite Reynolds and Marangoni numbers, *Phys. Fluids*, 9 (1997), 845–855.

- [6] Rider, W.J., Kothe, D.B., Reconstructing volume tracking, *J. Comput. Phys.*, 141 (1998), 112–152.
- [7] Lappa, M., Piccolo, C., Carotenuto, L., Mixed buoyant-Marangoni convection due to dissolution of a droplet in a liquid–liquid system with miscibility gap, *Eur. J. Mech. B*, 23 (2004), 781–794.
- [8] Perez de Ortiz, S.E., Sawistoski, H., Interfacial instability of binary liquid–liquid systems, I. Stability analysis, *J. Chem. Eng. Sci.*, 28 (1973), 2051–2061.
- [9] Fletcher, C.A.J., *Computational Techniques for Fluid-Dynamics*, Springer Verlag, Berlin, 1991.
- [10] Lappa, M., *Fluids, Materials and Microgravity: Numerical Techniques and Insights into the Physics*, Elsevier Science, Oxford, 2004.
- [11] Bassano, E., Numerical simulation of thermo-solutal-capillary migration of a dissolving drop in a cavity, *Int. J. Numer. Methods Fluids*, 41 (2003), 765–788.
- [12] Perez de Ortiz, S.E., Sawistowski, H., Interfacial instability of binary liquid–liquid systems, II. Stability behaviour of selected systems, *Chem. Eng. J.*, 28 (1973), 2063–2069.
- [13] Liang, T.B., Slater, M.J., Liquid–liquid extraction drop formation: Mass transfer and the influence of surfactant, *Chem. Eng. Sci.*, 45 (1990), 97–105.
- [14] Bekki, S., Vignes-Adler, M., Nakache, E., Adler, P.M., Solutal Marangoni effect. I. Pure interfacial transfer, *J. Colloid Interface Sci.*, 140 (1990), 492–506.
- [15] Bekki, S., Vignes-Adler, M., Nakache, E., Solutal Marangoni effect. II. Dissolution, *J. Colloid Interface Sci.*, 152 (1992), 314–324.
- [16] Agble, D., Mendes Tatsis, M.A., The effect of surfactants on interfacial mass transfer in binary liquid–liquid systems, *Int. J. Heat Mass Transfer*, 43 (2000), 1025–1034.
- [17] Agble, D., Mendes-Tatsis, M.A., The prediction of Marangoni convection in binary liquid–liquid systems with added surfactants, *Int. J. Heat Mass Transfer*, 44 (2001), 1439–1449.
- [18] Sterling, C.V., Scriven, L.E., Interfacial turbulence: Hydrodynamic instability and the Marangoni effect, *J. Am. Inst. Chem. Eng.*, 5 (1959), 514–523.
- [19] Hennenberg, M., Bisch, P.M., Vignes-Adler, M., Sanfeld, A., Mass transfer Marangoni and instability of interfacial longitudinal waves. I. Diffusional exchanges, *J. Colloid Interface Sci.*, 69 (1979), 128–137.
- [20] Hennenberg, M., Bisch, P.M., Vignes-Adler, M., Sanfeld, A., Mass transfer Marangoni and instability of interfacial longitudinal waves. II. Diffusional exchanges and adsorption–desorption processes, *J. Colloid Interface Sci.*, 74 (1979), 495–508.
- [21] Nakache, E., Dupeyrat, M., Vignes-Adler, M., Experimental and theoretical study of an interfacial instability at some oil–water interfaces involving a surface-active agent. I. Physicochemical description and outlines for a theoretical approach, *J. Colloid Interface Sci.*, 94 (1983), 120–127.
- [22] Lewis, J.B., Pratt, H.R.C., Oscillating droplets, *Nature*, 171 (1953), 1155–1156.
- [23] Konkachbaev, A., Morley, N.B., Stability and contraction of a rectangular liquid metal jet in vacuum environment, *Fusion Eng. Design*, 51/52 (2000), 1109–1114.
- [24] Tryggvason, G., Bunner, B., Esmaeeli, A., Juric, D., Al-Rawahi, N., Tauber, W., Han, J., Nas, S., Jan, Y.-J., A front tracking method for the computations of multiphase flow, *J. Comput. Phys.*, 169 (2001), 708–759.

Paper received: 2005-02-07

Paper accepted: 2005-03-15

